

Reversible O–O Bond Cleavage and Formation between Mn(IV)-Peroxo and Mn(V)-Oxo Corroles

Sun Hee Kim,[†] Hyejin Park,[†] Mi Sook Seo,[†] Minoru Kubo,[‡] Takashi Ogura,[‡] Jan Klajn,[§] Daniel T. Gryko,[§] Joan Selverstone Valentine,^{†,||} and Wonwoo Nam^{*,†}

Department of Bioinspired Science, Ewha Womans University, Seoul 120-750, Korea, Picobiology Institute, Graduate School of Life Science, University of Hyogo, Hyogo 678-1297, Japan, Institute of Organic Chemistry, Polish Academy of Sciences, Kasprzaka 44/52, 01-224 Warsaw, Poland, and Department of Chemistry and Biochemistry, UCLA, Los Angeles, California 90095-1569

Received July 27, 2010; E-mail: wwnam@ewha.ac.kr

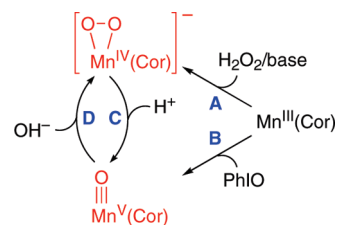
Abstract: Mn(IV)-peroxo and Mn(V)-oxo corroles were synthesized and characterized with various spectroscopic techniques. The intermediates were directly used in O–O bond cleavage and formation reactions. Upon addition of proton to the Mn(IV)-peroxo corrole, the formation of the Mn(V)-oxo corrole was observed. Interestingly, addition of base to the Mn(V)-oxo corrole afforded the formation of the Mn(IV)-peroxo corrole. Thus, we were able to report the first example of reversible O–O bond cleavage and formation reactions using in situ generated Mn(IV)-peroxo and Mn(V)-oxo corroles.

Dioxygen O–O bond-cleaving and bond-forming reactions occur at transition metal centers in a number of metalloenzymes. For example, heme and nonheme iron monooxygenases bind and activate O₂ to generate high-valent iron-oxo intermediates via O–O bond cleavage of iron(III)-peroxo precursors, [Fe(III)-O₂]⁺.¹ The O–O bond activation of iron–O₂ adducts has for that reason been intensively investigated using synthetic iron porphyrins to elucidate mechanisms of the iron-oxo intermediate formation over the past several decades (e.g., heterolysis vs homolysis).²

In the case of the O–O bond formation, the photosynthetic conversion of water into dioxygen occurs at the oxygen-evolving complex (OEC) in photosystem II (PS II); a manganese(V)-oxo intermediate has been implicated as an active species for the O–O bond formation.³ Very recently, Gao et al. reported an elegant result that the reaction of a Mn(V)-oxo corrole and hydroxide affords O₂ evolution; the O–O bond formation in the reaction was proposed to occur via nucleophilic attack of hydroxide ion on a Mn(V)-oxo moiety.⁴ Thus, O–O bond cleavage and O–O bond formation reactions in metalloenzymes have been successfully mimicked by biomimetic model studies. However, reversible O–O bond cleavage and formation between metal-O₂ and metal-oxo species has not been successfully modeled.⁵ Herein we report the first example of a reversible conversion between manganese-peroxo and -oxo corrole complexes via O–O bond cleavage and formation processes (see Scheme 1).

Addition of 1.2 equiv of H₂O₂ to a solution containing a manganese(III) corrole, Mn(TFMPC) (**1**, 3 × 10^{−2} mM) (TFMPC = 5,10,15-tris(3,5-trifluoromethylphenyl)corrolato trianion) (see structure in Supporting Information (SI), Figure S1), and tetramethylammonium hydroxide (TMAH, 20 equiv) in CH₃CN

Scheme 1



at 10 °C afforded the formation of a new intermediate, **2**, with absorption bands at 435 and 590 nm within 1 min (Scheme 1, reaction A; Figure 1 and SI, Figure S2 for UV–vis spectral changes). The intermediate was stable enough to be characterized by various spectroscopic methods (~10 min at 10 °C). The electrospray ionization mass spectrum (ESI MS) of **2** exhibited a prominent ion peak at a mass-to-charge ratio (*m/z*) of 1090.8, which corresponds to the mass and isotope distribution pattern of [Mn(TFMPC)(O₂)(CH₃CN)(CH₃OH)][−] (calculated *m/z* 1091.1; Figure 2a). The ESI MS of **2**, prepared with D₂O₂ in D₂O, showed the identical mass peak (SI, Figure S3), whereas **2**, prepared with H₂¹⁸O₂ in H₂¹⁶O, showed a mass peak at *m/z* 1094.8, which corresponds to [Mn(TFMPC)(¹⁸O₂)(CH₃CN)(CH₃OH)][−] (Figure 2a, inset). The 4 mass unit increase upon the substitution of ¹⁶O with ¹⁸O indicates that **2** contains an O₂ unit derived from H₂O₂. The X-band EPR spectrum of **2** exhibited a broad signal at *g* ≈ 4 (Figure 2b and SI, Figure S4 for EPR spectra taken during reactions), which we assign to a high-spin *S* = 3/2 Mn(IV) with a strong zero-field splitting.⁶ Taken together, the spectroscopic data provide strong evidence that **2**, generated in the reaction of **1** and H₂O₂ in the presence of base, is a high-spin Mn(IV) complex bearing an O₂ ligand, [Mn(IV)(TFMPC)(O₂)][−].⁷

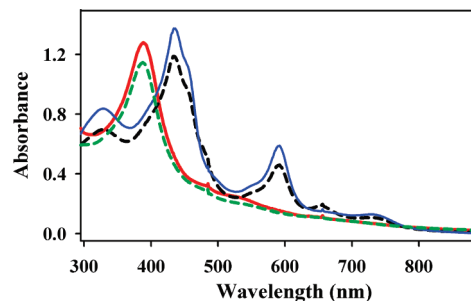


Figure 1. UV–vis spectra of **2** (solid blue line), **3** (solid red line), after addition of acid (20 equiv of HClO₄) to **2** (dashed green line), and after addition of base (20 equiv of TMAH) to **3** (dashed black line).

[†] Ewha Womans University.

[‡] University of Hyogo.

[§] Polish Academy of Sciences.

^{||} UCLA.

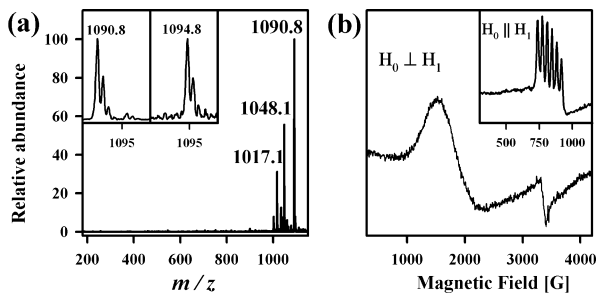


Figure 2. (a) ESI MS spectrum of **2**. Inset shows isotope distribution patterns for $2\text{-}^{16}\text{O}$ (left) and $2\text{-}^{18}\text{O}$ (right). The mass peaks at m/z 1017.1 and 1048.1 correspond to $[\text{Mn}(\text{TFMPC})(\text{CH}_3\text{O})]^-$ and $[\text{Mn}(\text{TFMPC})(\text{CH}_3\text{O})_2]^-$, respectively. (b) EPR spectrum of **2**. Inset shows a parallel mode X-Band CW-EPR spectrum of the starting $\text{Mn}^{\text{III}}(\text{TFMPC})$ complex. Also, see SI, Figure S4.

We then synthesized a $\text{Mn}(\text{V})$ -oxo corrole complex, **3**, by reacting **1** with 2.0 equiv of iodobenzene (PhIO) in CH_3CN at 10°C (Scheme 1, reaction B; Figure 1 and SI, Figure S5 for UV-vis spectral changes).⁸ The ESI MS of **3** exhibited a prominent ion peak at m/z 1002.1, whose mass and isotope distribution pattern corresponds to $\text{Mn}(\text{TFMPC})(\text{O})$ (calculated m/z 1002.1; Figure 3a). When **3** was prepared with isotopically labeled PhI^{18}O in the presence of H_2^{18}O , a mass peak corresponding to $\text{Mn}(\text{TFMPC})(^{18}\text{O})$ appeared at m/z 1004.2 (calculated m/z 1004.1; Figure 3a, inset). **3** is EPR silent (SI, Figure S4), suggesting a diamagnetic d^2 ($S = 0$) species as has been reported for other $\text{Mn}(\text{V})$ -oxo corrole and corrolazine complexes.^{8,9} The resonance Raman spectrum of **3**, measured in CH_3CN at -40°C with 442-nm laser excitation, displays an isotope sensitive band at 957 cm^{-1} , which shifts to 920 cm^{-1} upon introduction of ^{18}O (Figure 3b). The observed isotopic shift of -37 cm^{-1} with ^{18}O substitution is in close agreement with the value calculated for a $\text{Mn}-\text{O}$ diatomic oscillator (-42 cm^{-1}). The calculated force constant for the 957 cm^{-1} mode by a simple Hook's law is $6.7\text{ mdyne}/\text{\AA}$, which is consistent with triply bonded $\text{Mn}-\text{O}$ bonds in $\text{Mn}(\text{V})$ -oxo complexes.^{8c,9,10} Taken together, the spectroscopic data demonstrate that **3** is a $\text{Mn}(\text{V})$ -oxo corrole with a $\text{Mn}-\text{O}$ triple bond, $\text{Mn}^{\text{V}}(\text{O})(\text{TFMPC})$.

Remarkably, a reversible conversion between the $\text{Mn}(\text{IV})$ -peroxo and $\text{Mn}(\text{V})$ -oxo corroles was observed upon addition of acid and base (Scheme 1, reactions C and D); this reversible cycle could be repeated several times without showing a significant decrease of the absorption bands corresponding to the products. First, the $\text{Mn}(\text{IV})$ -peroxo complex, **2**, was converted to the $\text{Mn}(\text{V})$ -oxo complex, **3**, upon addition of HClO_4 (Scheme 1, reaction C); the full formation of **3** was confirmed by the UV-vis and EPR spectra of the resulting solution (Figure 1 and SI, Figure S4). In addition,

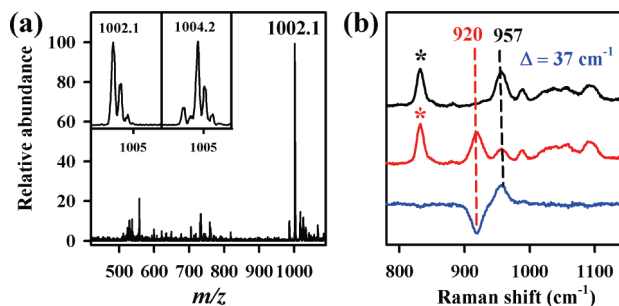
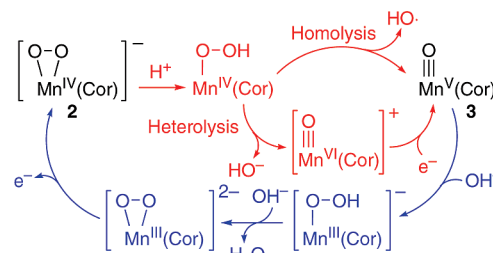


Figure 3. (a) ESI MS spectrum of the complex **3**. Inset shows isotope distribution patterns prepared with PhI^{16}O (left) and PhI^{18}O (right). (b) Resonance Raman spectra of **3** prepared with PhI^{16}O (black line) and PhI^{18}O (red line), and the difference spectrum of $3\text{-}^{16}\text{O}-3\text{-}^{18}\text{O}$ (blue line). The peaks marked with * are from solvent.

2 was converted to **3** by addition of benzoyl chloride (data not shown). It has been well-documented that the reactions of metal-peroxo species, including $\text{Mn}(\text{III})$ -peroxo porphyrins, with benzoyl chloride lead to formation of their corresponding high-valent metal-oxo species.¹¹ However, the $\text{O}-\text{O}$ bond cleavage mechanism of the putative $\text{Mn}(\text{IV})$ -OOH intermediate is not yet clear at this moment (see Scheme 2 for $\text{O}-\text{O}$ bond homolysis vs heterolysis). Nevertheless, to our knowledge, this is the first demonstration of the analogous conversion of a Mn -peroxo corrole to a Mn -oxo corrole upon protonation.

Scheme 2. Proposed Mechanisms of $\text{O}-\text{O}$ Bond Cleavage and Formation between Mn -Peroxo and -Oxo Corroles



In the $\text{O}-\text{O}$ bond formation reaction, addition of base to the $\text{Mn}(\text{V})$ -oxo complex, **3**, produced the $\text{Mn}(\text{IV})$ -peroxo complex, **2**, quantitatively (Scheme 1, reaction D; Figure 1). The formation of **2** was further confirmed by taking EPR and ESI MS of the resulting solution; a broad signal at $g \approx 4$ was observed in the EPR spectrum (SI, Figure S4). In ESI MS experiments, **2** prepared in the reaction of $\text{Mn}(\text{V})^{16}\text{O}$ and $^{16}\text{OH}^-$ contained an $^{16}\text{O}^{16}\text{O}$ group (SI, Figure S6). Similarly, **2** prepared in the reaction of $\text{Mn}(\text{V})^{18}\text{O}$ and $^{16}\text{OH}^-$ contained an $^{18}\text{O}^{16}\text{O}$ group (SI, Figure S6). These results demonstrate that the peroxo ligand in **2** was generated by the $\text{O}-\text{O}$ bond formation between the Mn -oxo moiety in **3** and the hydroxide ion, followed by a deprotonation of a hydroperoxo ligand by another hydroxide ion (Scheme 2).^{4,12} However, there is an electron missing in the proposed mechanism, and this is probably due to a greater stability of a $\text{Mn}(\text{IV})$ -peroxo corrole species under the reaction conditions.

In conclusion, we have synthesized and characterized new $\text{Mn}(\text{IV})$ -peroxo and $\text{Mn}(\text{V})$ -oxo corroles and used them in $\text{O}-\text{O}$ bond cleavage and formation reactions. We have also shown the first example of reversible $\text{O}-\text{O}$ bond cleavage and formation between high-valent metal-oxo and metal-peroxo species. Future studies will be focused on understanding mechanistic aspects involved in the $\text{O}-\text{O}$ bond cleavage and formation processes.

Acknowledgment. The research was supported by KOSEF/MEST of Korea through the CRI, WCU (R31-2008-000-10010-0), and GRL (2010-00353) Programs (to W.N. and J.S.V.), Grant-in-Aid for scientific research (C) (No. 21570171) and Priority Area (No. 477) (KAKENHI) and GCOE program (Picobiology) by MEXT, Japan (to T.O.), and Polish Ministry of Science and Higher Education (Contract 50611) (to D.T.G.).

Supporting Information Available: Experimental details and Figures S1–S6. This material is available free of charge via the Internet at <http://pubs.acs.org>.

References

- (1) Nam, W. *Acc. Chem. Res.* **2007**, *40*, 465. and review articles in the special issue.
- (2) (a) Groves, J. T. In *Cytochrome P450: Structure, Mechanism, and Biochemistry*; Ortiz de Montellano, P. R., Ed.; Kluwer Academic/Plenum Publishers: New York, 2005; pp 1–43. (b) Wertz, D. L.; Valentine, J. S. *Struct. Bonding (Berlin)* **2000**, *97*, 37–60. (c) Shaik, S.; Kumar, D.; de

- Visser, S. P.; Altun, A.; Thiel, W. *Chem. Rev.* **2005**, *105*, 2279–2328. (d) Nam, W. *Acc. Chem. Res.* **2007**, *40*, 522–531.
- (3) (a) McEvoy, J. P.; Brudvig, G. W. *Chem. Rev.* **2006**, *106*, 4455–4483. (b) Meyer, T. J.; Huynh, M. H. V.; Thorp, H. H. *Angew. Chem., Int. Ed.* **2007**, *46*, 5284–5304. (c) Romain, S.; Vigara, L.; Llobet, A. *Acc. Chem. Res.* **2009**, *42*, 1944–1953. (d) Barber, J. *Chem. Soc. Rev.* **2009**, *38*, 185–196.
- (4) Gao, Y.; Akermark, T.; Liu, J.; Sun, L.; Akermark, B. *J. Am. Chem. Soc.* **2009**, *131*, 8726–8727.
- (5) (a) Halfen, J. A.; Mahapatra, S.; Wilkinson, E. C.; Kaderli, S.; Young, V. G.; Que, L.; Zuberbühler, A. D.; Tolman, W. B. *Science* **1996**, *271*, 1397–1400. (b) Furutachi, H.; Hashimoto, K.; Nagatomo, S.; Endo, T.; Fujinami, S.; Watanabe, Y.; Kitagawa, T.; Suzuki, M. *J. Am. Chem. Soc.* **2005**, *127*, 4550–4551. (c) Lee, A. Q.; Streit, B. R.; Zdilla, M. J.; Abu-Omar, M. M.; DuBois, J. L. *Proc. Natl. Acad. Sci. U.S.A.* **2008**, *105*, 15654–15659. (d) Zdilla, M. J.; Lee, A. Q.; Abu-Omar, M. M. *Inorg. Chem.* **2009**, *48*, 2260–2268.
- (6) Kessissoglou, D. P.; Li, X.; Butler, W. M.; Pecoraro, V. L. *Inorg. Chem.* **1987**, *26*, 2487–2492.
- (7) The binding mode (e.g., side-on vs end-on) of the peroxo ligand in **2** is not determined yet, although several crystal structures of “side-on” Mn(III)-peroxo complexes bearing heme and nonheme ligands have been reported previously. It is also noted that peroxo O–O stretching vibrations by resonance Raman spectroscopy have never been observed in Mn-peroxo complexes. (a) VanAtta, R. B.; Strouse, C. E.; Hanson, L. K.; Valentine, J. S. *J. Am. Chem. Soc.* **1987**, *109*, 1425–1434. (b) Kitajima, N.; Komatsuzaki, H.; Hikichi, S.; Osawa, M.; Moro-Oka, Y. *J. Am. Chem. Soc.* **1994**, *116*, 11596–11597. (c) Seo, M. S.; Kim, J. Y.; Annaraj, J.; Kim, Y.; Lee, Y.-M.; Kim, S.-J.; Kim, J.; Nam, W. *Angew. Chem., Int. Ed.* **2007**, *46*, 377–380. (d) Annaraj, J.; Cho, J.; Lee, Y.-M.; Kim, S. Y.; Latifi, R.; de Visser, S. P.; Nam, W. *Angew. Chem., Int. Ed.* **2009**, *48*, 4150–4153.
- (8) PhIO has been often used as an oxidant in generating Mn(V)-oxo corroles: (a) Gross, Z.; Golubkov, G.; Simkhovich, L. *Angew. Chem., Int. Ed.* **2000**, *39*, 4045–4047. (b) Liu, H.-Y.; Lai, T.-S.; Yeung, L.-L.; Chang, C. K. *Org. Lett.* **2003**, *5*, 617–620. (c) Liu, H.-Y.; Yam, F.; Xie, Y. T.; Li, X. Y.; Chang, C. K. *J. Am. Chem. Soc.* **2009**, *131*, 12890–12891.
- (9) Mandimutsira, B. S.; Ramdhanie, B.; Todd, R. C.; Wang, H.; Zareba, A. A.; Czernuszewicz, R. S.; Goldberg, D. P. *J. Am. Chem. Soc.* **2002**, *124*, 15170–15171.
- (10) (a) Collins, T. J.; Powell, R. D.; Slebodnick, C.; Uffelman, E. S. *J. Am. Chem. Soc.* **1990**, *112*, 899–901. (b) MacDonnell, F. M.; Fackler, N. L. P.; Stern, C.; O’Halloran, T. V. *J. Am. Chem. Soc.* **1994**, *116*, 7431–7432. (c) Miller, C. G.; Gordon-Wylie, S. W.; Horwitz, C. P.; Strazisar, S. A.; Peraino, D. K.; Clark, G. R.; Weintraub, S. T.; Collins, T. J. *J. Am. Chem. Soc.* **1998**, *120*, 11540–11541.
- (11) (a) Watanabe, Y. In *The Porphyrin Handbook*; Kadish, K. M., Smith, K. M., Guillard, R., Eds.; Academic: New York, 2000; Vol. 4, Chapter 30, pp 97–117. (b) Groves, J. T.; Watanabe, Y. *Inorg. Chem.* **1986**, *25*, 4808–4810. (c) Groves, J. T.; Watanabe, Y.; McMurtry, T. J. *J. Am. Chem. Soc.* **1983**, *105*, 4489–4490.
- (12) Privalov, T.; Sun, L.; Akermark, B.; Liu, J.; Gao, Y.; Wang, M. *Inorg. Chem.* **2007**, *46*, 7075–7086.

JA1066465